ELSEVIER

Journal of Power Sources 108 (2002) 213–225

JOURNAL OF POWER SOURCES

www.elsevier.com/locate/jpowsour

Evaluation of thermodynamically favourable operating conditions for production of hydrogen in three different reforming technologies

Y.-S. Seo[a,*], A. Shirley[b], S.T. Kolaczkowski[b]

[a]*Korea Institute of Energy Research, 71-2 Jang-dong Yusung-gu Taejon, 305-343, South Korea*
[b]*Department of Chemical Engineering, University of Bath, Bath BA2 7AY, UK*

Received 6 August 2001; accepted 2 January 2002

Abstract

With the aid of thermodynamic analysis using AspenPlus™, the characteristics of three different types of reforming process are investigated. These include: steam-methane reforming (SMR), partial oxidation (POX) and autothermal reforming (ATR). Thereby, favourable operating conditions are identified for each process. The optimum steam-to-carbon (S:C) ratio of the SMR reactor is found to be 1.9. The optimum air ratio of the POX reactor is 0.3 at a preheat temperature of 312 °C. The optimum air ratio and S:C ratio of the ATR reactor are 0.29 and 0.35, respectively at a preheat temperature of 400 °C. Simulated material and energy balances show that the CH_4 flow rates required to generate 1 mol s^{-1} of hydrogen are 0.364 mol s^{-1} for POX, 0.367 mol s^{-1} for ATR and 0.385 mol s^{-1} for the SMR. These results demonstrate that the POX reforming system has the lowest energy cost to produce the same amount of hydrogen from CH_4.

Keywords: Hydrogen; Steam reforming; Partial oxidation; Autothermal reforming; Thermodynamic analysis; Material and energy balance

1. Introduction

Today, hydrogen has emerged as an alternative clean energy source to existing fossil fuels [1]. Hydrogen can be directly combusted in an internal combustion engine or electrochemically converted to electricity in a fuel cell system. Neither of these processes produces carbon dioxide, soot or carbon monoxide. Vehicles which employ a fuel cell and a hydrocarbon fuel require an efficient and safe hydrogen generator. Such devices have been intensively developed [2–4]. Such activity is connected with increasing research world-wide in the field of polymer electrolyte membrane (PEM) fuel cells [5,6].

In general, technologies for the production of hydrogen from methane are based on one of the following three processes: steam-methane reforming (SMR); partial oxidation (POX); autothermal reforming (ATR). The SMR technology is the oldest and most widely used, but it has a disadvantage of slow start-up, which makes it more suitable for a stationary system rather than for a mobile system. Recently, catalytic POX reforming [7–10] and ATR reforming [11,12] appear to have attracted much interest. The POX consists of sub-stoichiometric oxidation of methane, while the ATR integrates POX with SMR. In general, both POX and ATR have low energy requirement and high gas-space velocity [13].

A reforming system is generally comprised of a pretreatment process, a reforming reactor, a shift reactor and a gas-purification process. A reforming system to produce hydrogen from liquefied natural gas (LNG) requires a desulphurisation unit as a pretreatment process. LNG usually contains a very low level of sulphur (lower than 10 ppm), but this sulphur can deactivate severely the catalysts used in reforming reactors and shift reactors, especially in the case of low catalyst operation temperatures. At less than 600 °C, the poisoning of catalysts by sulphur compounds becomes more significant. In general, the desulphurisation unit is installed before the reforming reactor. If the operating temperature of the reforming reactor is sufficiently high (more than 700 °C), however, then the unit can be installed between the reforming reactor and the shift reactor. The pretreatment unit has been excluded from the thermodynamic analysis performed in this study.

Synthesis gas produced from reforming reactions contains an appreciable amount of carbon monoxide. Therefore, it is further processed in a water–gas shift reactor where the carbon monoxide is converted into hydrogen by reaction

* Corresponding author. Tel.: +82-42-860-3612; fax: +82-42-860-3134.
E-mail address: ysseo@kier.re.kr (Y.-S. Seo).

0378-7753/02/$ – see front matter
PII: S0378-7753(02)00027-7

with steam. Water–gas shift reactors can be classified as one of two types according to their working temperature. A high-temperature shift reactor is operated at around 400 °C, while a low-temperature shift reactor is operated at around 200 °C.

After the shift reactor, the CO concentration is lower than 1.0%. In fact, many applications which utilise hydrogen require a lower CO concentration than this. For example, a PEM fuel cell (PEMFC) requires hydrogen with a CO concentration that is below 20 ppm [14]. To this end, the synthesis gas should be further cleaned to remove CO. This can be achieved by using preferential oxidation, selective methanation, adsorption or a membrane. Finally, pure hydrogen gas can be directly fed into a fuel cell, or a storage tank.

The purpose of this paper is to identify thermodynamically favourable operating conditions at which methane may be converted to hydrogen in the SMR, POX and ATR processes. First of all, the characteristics of each reforming reactor have been investigated by performing a thermodynamic equilibrium analysis for the products and reactants. This part of the investigation provides knowledge on how operating parameters such as input conditions of reactants and thermodynamic conditions in the reforming reactor affect the equilibrium. Each reforming reactor is expected to have its own favourable operating characteristics. As equilibrium is assumed, these may vary in a practical situation. Nevertheless, the results provide a valuable indication of the starting point for experimental research.

Next, the thermal energy required in each of the reforming systems, (which comprise a reforming reactor, a water–gas shift reactor, a steam generator and a heat exchanger), has been evaluated by performing material and energy balances for each system. The consumption of thermal energy is a key issue in the design of a reforming system.

2. Simulation methods

The thermodynamic equilibrium in a reforming reactor can be calculated in two ways. One is to use equilibrium constants, the other is to minimise the Gibbs free energy. It is well known that the former approach makes it difficult to analyse the solid carbon (graphite) which can be generated during the reforming process. Therefore, the method of minimising the Gibbs free energy is normally preferred in fuel-reforming analysis [15]. This method has been adopted in the study reported here. The following are operating parameters of the reformer: (i) preheat temperature of reactants; (ii) composition and flow rate of air, methane and water; (iii) pressure of the reforming reactor; (iv) temperature of the reforming reactor.

For given operating conditions, the equilibrium temperature of the reactor and the equilibrium compositions have been calculated. This calculation can be made with any commercially available software. In this study, AspenPlus™ [16] was used. In the simulation, the mole fraction composition of air was assumed to be 0.2095 O_2 and 0.7905 N_2. To analyse the reforming reactor effectively, two parameters, the air ratio and the steam-to-carbon ratio (S:C) were used. The former refers to the relationship between air and methane flow rates and the latter refers to the relationship between steam and methane flow rates. The parameters can be written as follows:

$$\text{air ratio} = 0.5\left(\frac{\text{molar flow rate of } O_2}{\text{molar flow rate of } CH_4}\right) \quad (1)$$

$$\text{steam-to-carbon ratio (S : C)} = \frac{\text{molar flow rate of steam}}{\text{carbon molar flow rate in } CH_4} \quad (2)$$

As a general goal, it is desirable to achieve a conversion which is as high as possible within allowable operating conditions. But in many cases if the fractional conversion approached a value of 1.0, then this could damage the durability of the reactor system. The durability of the reformer is governed by the thermal durability of the reforming catalysts and the deactivation of the catalysts by coke formation. In this analysis, the maximum allowable temperature of the catalysts is assumed to be 800 °C for all three reforming reactors. In reality, a certain catalyst for a reforming system might be able to be used at higher temperatures, but most commercially available catalysts have been operated at less than 800 °C to secure their thermal durability. Therefore, it is necessary to determine favourable operating conditions for each of the reforming reactors. These are defined as conditions at which the fractional conversion is more than 0.99 while the durability of the reformer system is secured.

Material and energy balances are then solved for each system, making use of AspenPlus™ software. It is assumed that each system consists of a steam generator, a preheating system, a reforming reactor, a heat exchanger and a water–gas shifter reactor. In order to compare the utilisation of thermal energy in the three systems, the operating conditions for each system are set to the favourable operating conditions identified in the equilibrium simulation. By comparing the energy utilisation in each reforming system, it is possible to evaluate that which system has the lowest energy cost.

3. Simulation results and discussion

3.1. Equilibrium analysis

3.1.1. SMR

To analyse the thermodynamic equilibrium of the SMR reactor, the general reforming reaction mechanism can be written in the following way:

$$CH_4 + \beta H_2O \Rightarrow \text{products} \quad (3)$$

The products can be CH_4, H_2O, H_2, CO, CO_2, C(s), H, O, OH, HO_2, HCO, CH or CH_2. C(s) refers to solid carbon (graphite) and H, O, OH, HO_2, HCO, CH, CH_2 are radicals

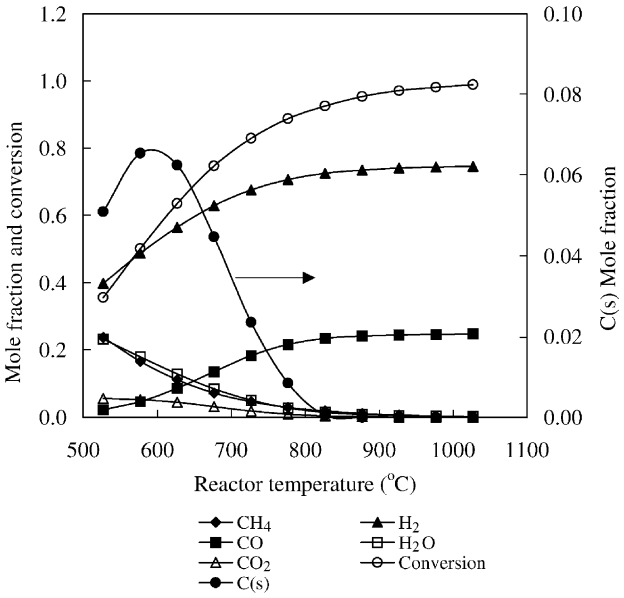

Fig. 1. Effect of reactor temperature on equilibrium compositions and conversion in SMR reactor. Reactor pressure, 1.0 bar; S:C ratio, 1.0.

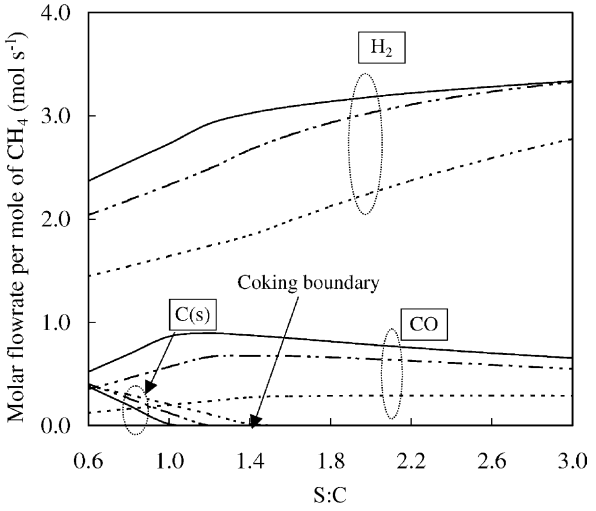

Fig. 2. Effect of S:C on equilibrium compositions in SMR reactor. Reactor pressure: 1.0 bar. Reactor temperature: (- - -) 600 °C; (– - - –) 700 °C; (—) 800 °C.

that could be produced in the reforming reaction. In the simulations, the concentration of radicals is found to be negligible compared with those of the other products. The stoichiometric coefficient, β, for H_2O is varied from 0.6 to 3.0, which corresponds to a S:C ratio range of 0.6–3.0. As the SMR is very endothermic, heat-transfer from the outside of the reactor controls the temperature of the SMR reactor. In this simulation, the temperature of the SMR reactor is varied in the range 500–1000 °C.

The reactor temperature is found to affect significantly the equilibrium compositions and, therefore, the conversion (see Fig. 1). As the reactor temperature is raised from 600 to 800 °C, the conversion increases from 0.56 to 0.90. If the operating temperature of the reactor is limited to less than 800 °C in order to maintain thermal durability of the catalyst, then it can be seen that it is difficult to obtain a satisfactory conversion that is greater than 0.99.

The reactor temperature also significantly affects the formation of solid carbon, C(s). It is generated at temperatures of less than 850 °C with a S:C of 1.0 and at 1.0 bar reactor pressure. This implies that in order to avoid coke formation, the reactor temperature should be maintained at temperatures that are greater than 850 °C. On the other hand, keeping the reactor temperature above 850 °C is likely to damage the thermal durability of the catalyst. Therefore, it is necessary to change other operating parameters in order to suppress coke formation in the temperature region below 850 °C. The formation of solid carbon might be caused by the following Boudouard reaction [17].

$$2CO \Rightarrow C + CO_2 \quad (4)$$

This is supported by the fact that CO_2 is generated only in the region in which C(s) exists (see Fig. 1). It is found, however, that the equilibrium compositions in the SMR reactor are independent of the preheat temperature of the reactants, as long as the reactor temperature is fixed at a certain value. This is because the temperature of the SMR reactor is determined by the external heat-transfer to the reactor. For the purpose of the thermodynamic calculations, the reactor temperature of the SMR reactor is given as an input parameter; hence the preheat temperature affects only the heat duty that is transferred to the SMR reactor.

The simulation results of the SMR reactor in terms of the S:C ratio are illustrated in Figs. 2 and 3. The data in Fig. 2 show that the formation of C(s) is strongly affected by the value of S:C. The coking boundary is defined as the limit condition within which the coke is generated. The coking boundary in the SMR reactor moves toward lower S:C values as the reactor temperature is raised. For example, if the reactor temperature is increased from 600 to 800 °C,

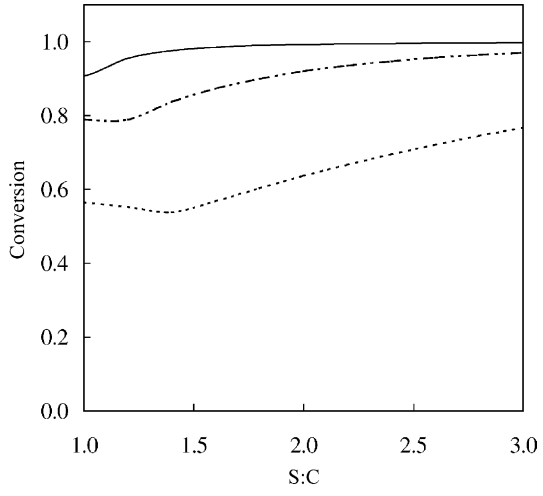

Fig. 3. Effect of S:C on conversion in SMR reactor. Reactor pressure: 1.0 bar. Reactor temperature: (- - -) 600 °C; (– - - –) 700 °C; (—) 800 °C.

the coking boundary moves from a S:C of 1.4 to 1.0. These results demonstrate that the formation of solid carbon can be avoided by increasing the reactor temperature and/or the S:C ratio. The maximum reactor temperature is restricted, however, by the thermal durability of the catalysts and the maximum value of S:C is limited according to the energy cost of the reactor system. A higher S:C incurs a higher energy cost because of the extra steam generation required. The molar flow rate of H_2 is increased and the molar flow rate of CO is decreased by increasing the S:C ratio. This is an advantage with using a higher S:C ratio.

The effects of the S:C ratio on the conversion of the SMR reactor at three reactor temperatures, 600, 700 and 800 °C, are shown in Fig. 3. Generally, the conversion is improved as the S:C value is increased, but in case of a low reactor temperature, viz., 600 °C, the complete conversion is difficult to obtain within a reasonable S:C range. If a SMR reactor is operated at 700 °C, the S:C should be maintained at greater than 2.5 in order to achieve a conversion of 0.95. In case of a reactor temperature of 800 °C, the conversion becomes greater than 0.95 when the S:C is more than 1.2. These simulation results demonstrate that both the S:C and the reactor temperature strongly affect conversion in the SMR reactor.

A sensitivity analysis has also been conducted with regard to the effect of varying the pressure of the SMR reactor. The effects of varying the pressure on the equilibrium compositions and the conversion in the SMR reactor are shown in Fig. 4. The simulation results reveal that the pressure of the reactor is one of the critical factors which affect the equilibrium state of the SMR reactor. As the pressure is increased, the conversion and mole fractions of H_2 and CO are rapidly reduced. Conversely, the mole fraction of H_2O increases with pressure. These results demonstrate that it is desirable to keep the pressure of the SMR reactor as low as possible. It is interesting to note,

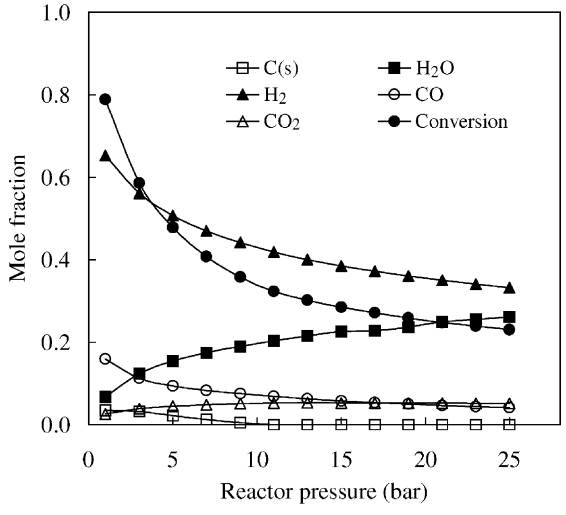

Fig. 4. Effects of the pressure on the equilibrium compositions and conversion in SMR reactor. Reactor temperature, 700 °C; S:C ratio, 1.0.

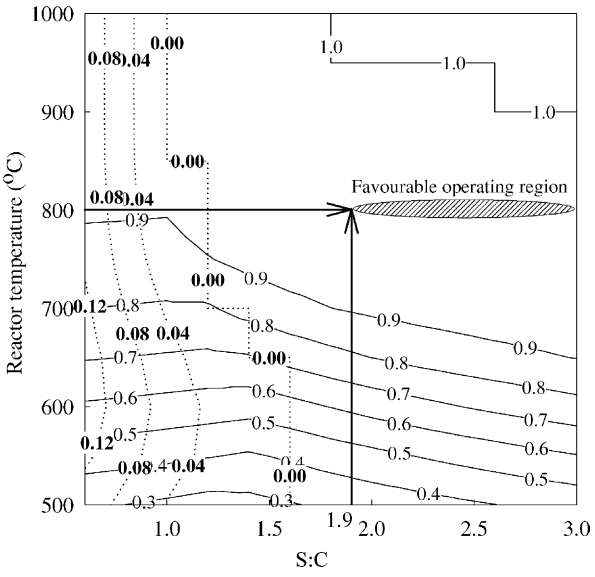

Fig. 5. Contour diagram of C(s) and conversion with regard to both reactor temperature and S:C ratio in SMR reactor. Reactor pressure, 1.0 bar; (- - -) C(s) mole fraction; (—) conversion.

however, that as the pressure is decreased, there is an increase in C(s) formation.

Favourable operating conditions in the SMR reactor can be ensured by the proper combination of reactor temperature, reactor pressure and S:C ratio. In the simulation of an SMR reactor, the pressure is fixed at 1.0 bar. A contour diagram that combines the conversion and C(s) mole fraction in terms of both the air ratio and the reactor temperature is shown in Fig. 5. This diagram provides the operation conditions that simultaneously satisfy the two conditions of no coke formation and a conversion of over 0.99 at a fixed reactor temperature of 800 °C. The result is shown in the Fig. 5 with thick arrows. Using this simulation, the optimum S:C ratio of the SMR reactor is found to be 1.9 or more. Under these operation conditions, the conversion of the reactor is calculated to be 0.99.

3.1.2. POX

The general reaction mechanism for the thermodynamic analysis of the POX reforming rector can be written as follows:

$$CH_4 + \alpha O_2 + 3.77\alpha N_2 \Rightarrow \text{products} \quad (5)$$

The stoichiometric coefficient of O_2, α, is varied from 0.0 to 1.2, which corresponds to an air ratio range of 0.0–0.6. The POX reforming reactor is modelled at adiabatic conditions during the calculation of the equilibrium state, which means that there is no heat-transfer to or from the POX reactor.

First, the POX reactor is simulated for various air ratios and reactant input temperatures. The equilibrium compositions of CH_4, C(s), H_2, CO, CO_2, H_2O are shown in Fig. 6 and have been calculated as a function of the air ratio over the range 0.0–0.6 at a preheat temperature of 200 °C and a

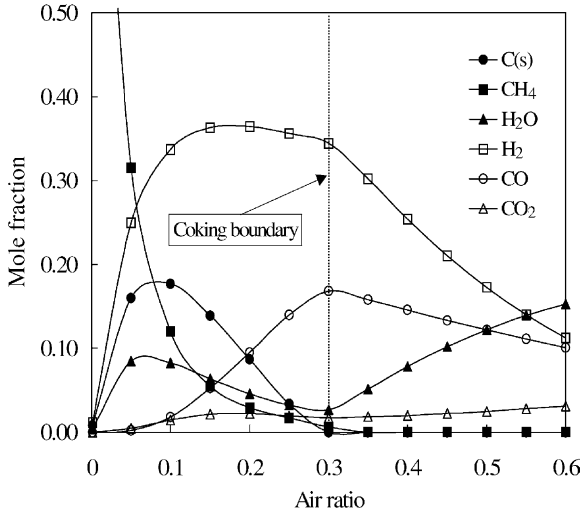

Fig. 6. Equilibrium composition of POX reactor with regard to air ratio. Preheat temperature of reactants (methane and air), 200 °C; reactor pressure, 1.0 bar.

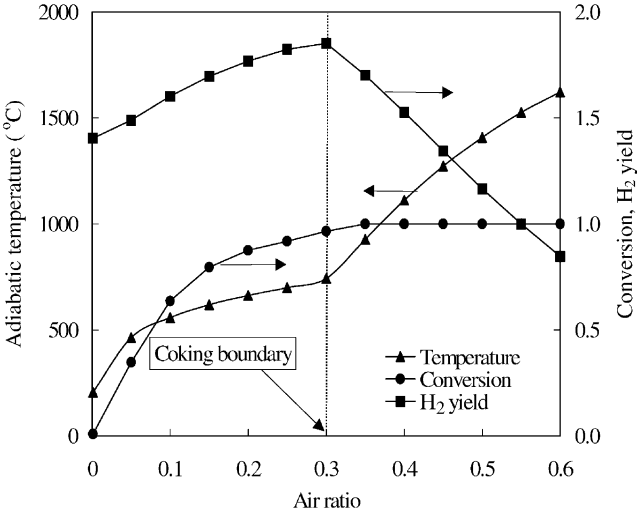

Fig. 7. Adiabatic temperature, conversion of methane and H_2 yield of POX reactor with regard to air ratio. Preheat temperature of reactants (methane and air), 200 °C; reactor pressure, 1.0 bar.

reactor pressure of 1.0 bar. The results have been sorted into two groups based on a coking boundary. The coking boundary is situated at an air ratio of 0.3. In the coking region, which corresponds to an air ratio range of 0.0–0.3, H_2 increases steeply with increasing air ratio. C(s) increases to a peak near an air ratio of 0.1, reduces gradually and finally drops to zero at an air ratio of 0.3. For an air ratio of more than 0.3, however, the H_2 concentration reduces rapidly with increasing air ratio, which leads to increased H_2O concentration. The CO also reduces with increased air ratio, but its rate of decrease is less than that of H_2. The decrease of H_2 and CO is contrary to the original aim of converting CH_4 completely into H_2 and CO. Therefore, operation of the POX reactor with an air ratio of greater than 0.3 is clearly undesirable.

The H_2 yield, conversion and adiabatic temperature of the POX reactor in terms of the air ratio are shown in Fig. 7. The H_2 yield is defined as:

$$H_2 \text{ yield} = \frac{[H_2]_{out}}{[CH_4]_{in} - [CH_4]_{out}} \quad (6)$$

The coking boundary is shown at an air ratio of 0.3 in the Fig. 7. At the coking boundary, the behaviour of both the H_2 yield and the adiabatic temperature drastically changes. The H_2 yield increases steadily with the air ratio in the region with the coking, but it decreases with the air ratio in the region without coke formation and this results in a lower quality of reformate. It is desirable for the reformed gas to contain as high a level of H_2 as possible. The adiabatic temperature of the reactor rises with the air ratio, but it increases more steeply in the region without coke formation. At the coking boundary, the adiabatic temperature and the H_2 yield are 743 and 0.97 °C, respectively.

The preheat temperature of reactants (CH_4 and air) can exert an important effect on the POX reactor. Reactants entering the POX reactor should be heated to a certain temperature to sustain the catalytic reaction of the reforming catalysts. The calculated results of the POX reactor with regard to the preheat temperature are presented in Figs. 8 and 9. The mole fractions of H_2 and CO are increased as the preheat temperature becomes higher (see Fig. 8). The behaviour of C(s) is, however, somewhat different from that of H_2 and CO. In the region of a very low air ratio (less than 0.1), the mole fraction of C(s) rises with increasing preheat temperature. By contrast, the mole fraction of C(s) reduces with the preheat temperature when the air ratio becomes greater than 0.1. The boundary line of coke formation hardly changes with respect to the preheat temperature. This demonstrates that to increase only the preheat temperature of reactants is not an effective way to avoid coke formation.

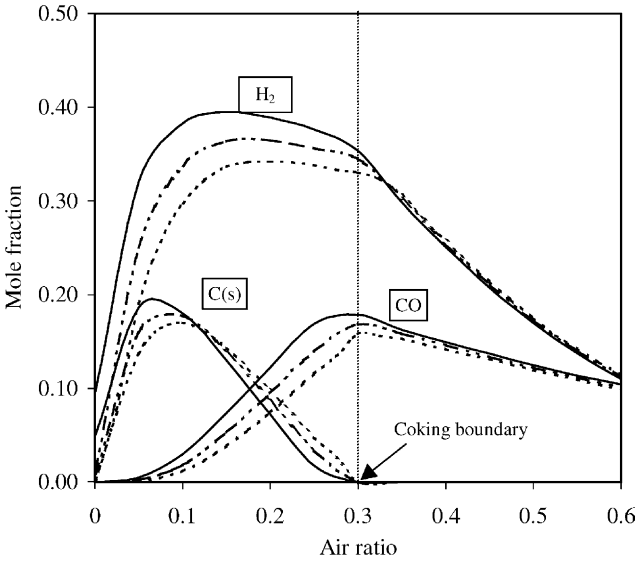

Fig. 8. Effects of preheat temperature of reactants on equilibrium compositions in POX reactor. Reactor pressure: 1.0 bar. Preheat temperature: (- - -) 20 °C; (– - - –) 200 °C; (—) 400 °C.

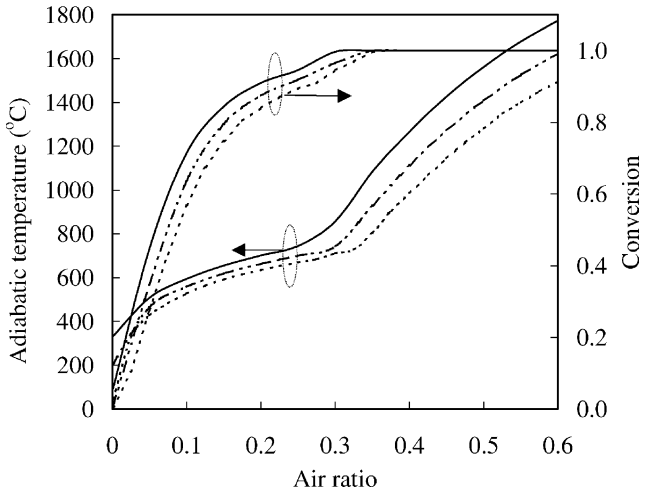

Fig. 9. Effects of preheat temperature of reactants on adiabatic temperature of POX reactor and conversion. Reactor pressure: 1.0 bar. Preheat temperature: (- - -) 20 °C; (– - - –) 200 °C; (—) 400 °C.

With an air ratio of more than 0.3, the mole fractions of H_2 and CO are hardly affected by the preheat temperature of the reactants. This trend becomes clearer as the air ratio is increased beyond 0.4.

The effects of the preheat temperature on the conversion and the adiabatic temperature of the POX reactor are shown in Fig. 9. Increasing the input temperature of the reactants causes both the conversion and the adiabatic temperature of the reactor to increase. To improve the conversion of the reformer, it is desirable to heat the reactants to a higher temperature, but this increases the adiabatic temperature of the POX reactor, which may cause deactivation of the catalysts. For example, the adiabatic temperature increases from 670 to 857 °C when the preheat temperature of the reactants is raised from 20 to 400 °C at an air ratio of 0.3. In the case of an air ratio of greater than 0.3, the adiabatic temperature rises steeply to more than 800 °C when the air ratio is increased by only a small amount. In reality, in order to operate the reactor with a high flow rate of reactants, it is necessary to heat the reactants sufficiently to maintain catalytic reaction. This thermodynamic analysis implies, however, that an excessive increase of the preheat temperature may cause the deactivation of the catalysts due to sintering at high-temperature.

To determine favourable operating conditions for the POX reactor, the C(s) formation, adiabatic reactor temperature and conversion have been calculated in terms of the air ratio and preheat temperature. The contour diagram that combines these results is given in Fig. 10. Favourable operation conditions are defined as those which simultaneously achieve no coke formation, an adiabatic reactor temperature of less than 800 °C and a conversion of over 0.99. These are indicated in Fig. 10 by the thick arrows. The optimum air ratio of the POX reactor is 0.3 at a preheat temperature of 312 °C. Under these operating conditions, the conversion of the reactor is calculated to be 0.99.

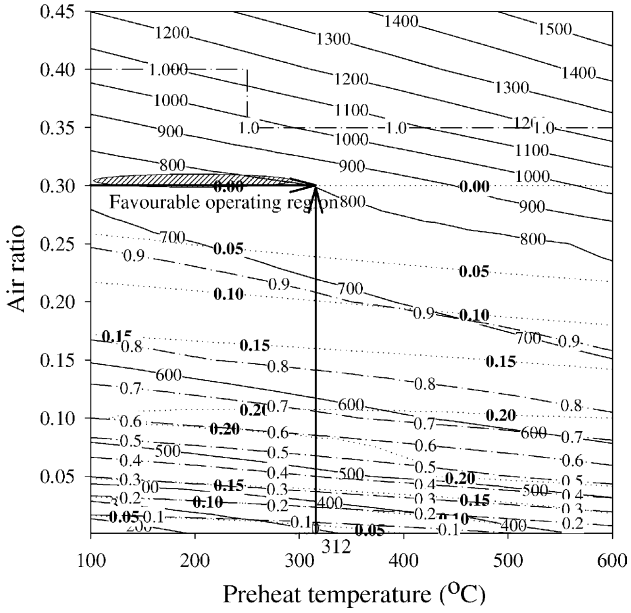

Fig. 10. Contour diagram of C(s), conversion and reactor temperature with regard to both air ratio and preheat temperature in POX reactor. Reactor pressure, 1.0 bar; (- - -) C(s) mole fraction; (– - –) conversion; (—) adiabatic reactor temperature (°C).

The preheat temperature of reactants is one of key operating parameters in the POX reactor. Thermodynamic analysis of the POX reactor shows that to increase the preheat temperature at a fixed air ratio makes both the reactor temperature and the conversion higher (see Fig. 10). If the temperature of catalyst is to be controlled within 800 °C, however, the air ratio should be altered to a lower value with increasing preheat temperature. When operating at a preheat temperature of over 312 °C, the formation of coke is inevitable if the reactor temperature is to be maintained at less than 800 °C. On the other hand, at a fixed preheat temperature, the conversion and the reactor temperature both increase with the air ratio, while the C(s) mole fraction is reduced. The favourable operating region in terms of the air ratio and preheat temperature is designated by the hatched area in Fig. 10.

3.1.3. ATR

The general reaction mechanism for the thermodynamic analysis of the ATR reactor can be written as follows:

$$CH_4 + \alpha O_2 + \beta H_2O + 3.77\alpha N_2 \Rightarrow \text{products} \quad (7)$$

The stoichiometric coefficient of O_2, α, is varied from 0.0 to 1.0, which corresponds to an air ratio range of 0.0–0.5. For each value of the air the ratio, the stoichiometric coefficient of H_2O, β, is varied from 0.0 to 1.2, which corresponds to a S:C ratio range of 0.0–1.2. As with the POX system, the ATR reactor is maintained under adiabatic conditions, which means that there is no heat-transfer to or from the reactor. The adiabatic temperature of the reactor is calculated with given input conditions of air ratio, S:C ratio, preheat temperature and reactor pressure.

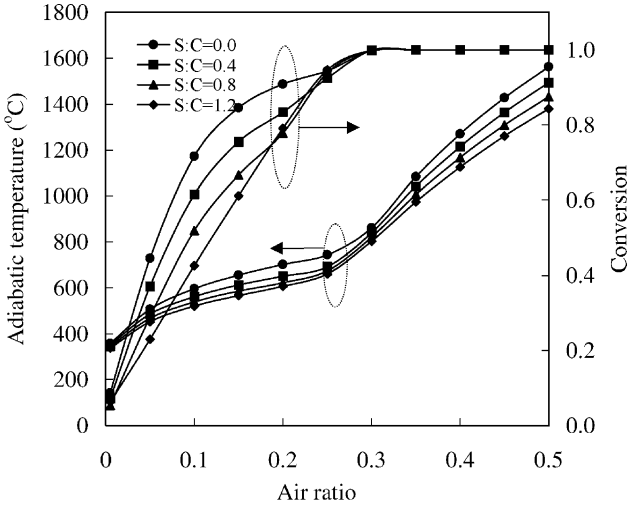

Fig. 11. Effect of air ratio and S:C ratio on adiabatic temperature and conversion in ATR reactor. Preheat temperature, 400 °C; reactor pressure, 1.0 bar.

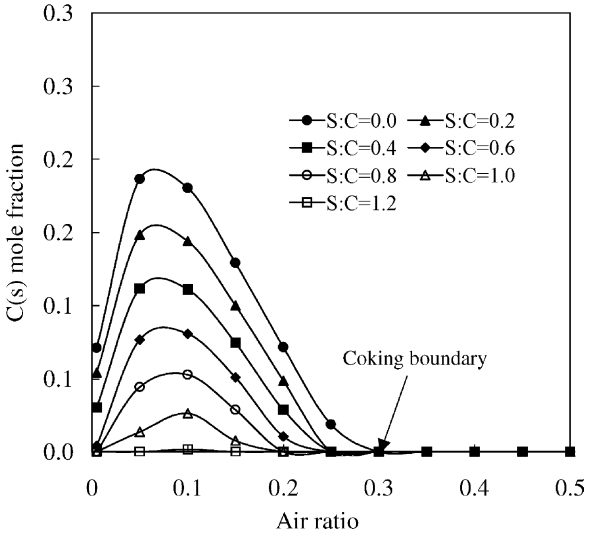

Fig. 12. Effect of air ratio and S:C ratio on C(s) formation in ATR reactor. Preheat temperature, 400 °C; reactor pressure, 1.0 bar.

The adiabatic temperature and the conversion in the ATR reactor in terms of the air ratio and the S:C ratio are shown in Fig. 11. The air ratio significantly affects the conversion and the adiabatic temperature. Conversion rapidly increases with the air ratio and reaches 1.0 at an air ratio of 0.3. For air ratios greater than 0.3, the adiabatic temperature continues to increase although the conversion remains at 1.0. This is due to oxidation of H_2 and CO into H_2O and CO_2 by excessive O_2 supply. The S:C ratio also affects both the conversion and the adiabatic temperatures of the ATR reactor. As the S:C ratio increases at a fixed air ratio, the conversion becomes lower and the adiabatic temperature decreases. When steam is supplied to the ATR reactor, the steam reforming reaction occurs, which is a strongly endothermic reaction. Therefore, a higher S:C results in a lower reactor temperature. As a result of the lower reactor temperature, the conversion is reduced.

The C(s) formation as a function of S:C ratio and air ratio is presented in Fig. 12. A higher S:C shifts the coking boundary to a lower air ratio and also reduces coke formation. As an example, the coking boundary moves from an air ratio of 0.3 to 0.2 if the S:C increases from 0.0 to 1.0. For a S:C of over 1.2, no coke is generated at any value of the air ratio. To avoid coke formation at a given air ratio, the optimum S:C can be derived from these results. The effects of the air ratio and S:C on the equilibrium compositions have also been investigated (see Fig. 13). The molar flow rates of H_2 and CO peak at an air ratio of 0.25 and 0.3, respectively. As S:C increases, the H_2 molar flow rate increases but, conversely, the CO mole flow rate decreases. This demonstrates that a higher S:C ratio causes the H_2:CO ratio to increase. On the other hand, if the air ratio is increased above 0.25, the H_2 molar flow rate drops more steeply when compared with the decrease in the CO molar flow rate. This is due to faster oxidation of H_2 than CO in the region of high air ratio.

To determine favourable operating conditions of the ATR reactor, the C(s) formation, adiabatic reactor temperature and conversion have been calculated in terms of the S:C ratio and air ratio. Contour diagrams that represent the results of these calculations are presented in Fig. 14. In the simulation to find the favourable operating conditions of the ATR reactor, the reactor pressure and the preheat temperature are set to 1 bar and 400 °C, respectively. From Fig. 14, the favourable operating conditions of the ATR reactor can be determined that simultaneously satisfy the requirements of no coke formation, a reactor temperature of 800 °C and a conversion of over 0.99. As a result, favourable operating conditions for the ATR reactor are found to be an air ratio of 0.29 and a S:C ratio of 0.35 at a preheat temperature of 400 °C. These conditions are shown in the Fig. 14 with thick arrows. The S:C ratio for this favourable operating region

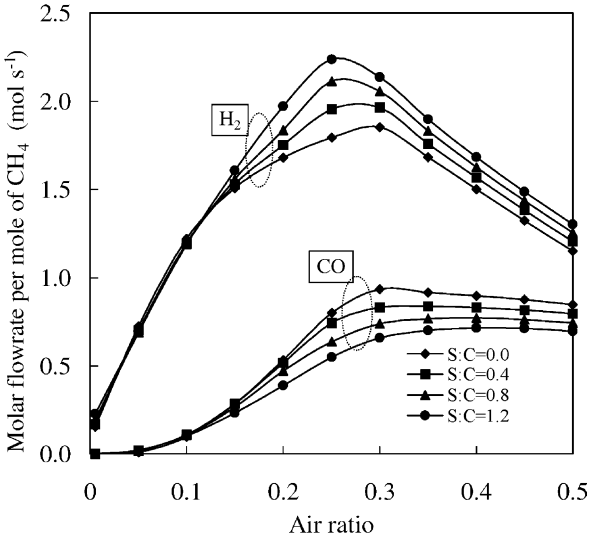

Fig. 13. Effect of air ratio and S:C ratio on mole fractions of H_2 and CO in ATR reactor. Preheat temperature, 400 °C; reactor pressure, 1.0 bar.

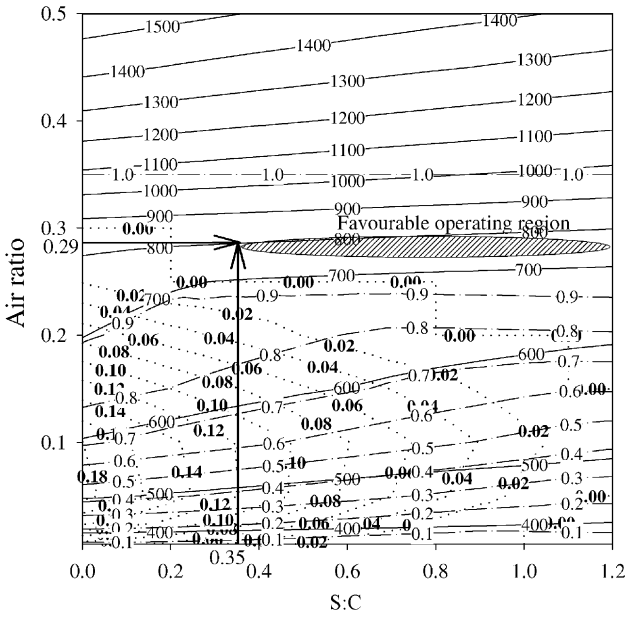

Fig. 14. Contour diagram of C(s), conversion and reactor temperature with regard to both air ratio and S:C ratio in ATR reactor. Reactor pressure, 1.0 bar; (- - -) C(s) mole fraction; (– – –) conversion; (—) adiabatic reactor temperature (°C).

can be extended beyond 0.35 when the air ratio is kept at 0.29. The hatched area shows the favourable operating region. It can be seen that the optimum air ratio exists within a very narrow range. On the other hand, the S:C ratio for the favourable operating region can be any value above 0.35. Nevertheless, the best S:C should be the lowest value, that is, 0.35, because a higher S:C incurs a greater energy cost in supplying the corresponding steam. In Table 1, a summary is provided of the favourable operating conditions for the three reforming reactors, SMR, POX and ATR. These data are used later to calculate the thermal energy requirements of each reforming system.

3.2. Analysis of thermal energy

It is useful to determine which of the three reforming systems is more efficient in terms of energy cost to generate a given amount of hydrogen. It is difficult, however, to compare each reforming system exactly because each has a different configuration to the others. For example, the SMR reforming system has a heat exchanger to supply the heat to the reforming reactor, while the POX and ATR reforming systems do not need any heat exchanger. Furthermore, the practical systems are composed of very complicated configurations in order to recover any available energy. In this study, the output flow rate of hydrogen is set to 1.0 mol s^{-1} in order to compare the three systems with one another. To this end, the calculation is iterated, changing the flow rate of reactants as an independent variable until the output flow rate of hydrogen reaches 1.0 mol s^{-1}. The data listed in Table 1 are used as input conditions for each reforming reactor. In order that the CH_4 conversion of each reforming reactor is kept at exactly the same level, viz., $0.991 \pm 0.1\%$, the input conditions of the ATR reactor have to be slightly adjusted. The air ratio and S:C ratio in the ATR reactor are adjusted from 0.29 and 0.35, to 0.285 and 0.2, respectively. On the other hand, a water–gas shift reactor is normally used in practical systems to convert CO generated from the reforming reactor into hydrogen. Therefore, this simulation employs a water–gas shift reactor behind the reforming reactor.

Table 1
Favourable operation conditions of three reforming systems

	SMR	POX	ATR
Air ratio	–	0.3	0.29
S:C ratio	1.9	–	0.35
Preheat temperature (°C)	400	312	400
Reactor temperature (°C)	800	800	800
Reactor pressure (bar)	1.0	1.0	1.0
Fractional conversion of CH_4	0.99	0.99	1.00

The configuration of each reforming system is described in Tables 2–4. Basically, each system comprises a steam generator, a heater, a reforming reactor, a heat exchanger and a shift reactor. The input conditions of air, CH_4 and water are set to 20 °C and 1 bar. Steam generators are used to generate the steam required for both the reforming reactor and the shift reactor. All steam generators are run at 103 °C. The S:C data obtained through analysis of the favourable operating conditions (Table 1) are used to determine the water flow rate for each reforming reactor. The water flow rate for the shift reactor is determined based on the complete conversion of CO to hydrogen. Equilibrium analysis of the shift reactor shows that the S:C should be 2.0 to obtain a CO conversion of 0.99 or more. Therefore, the S:C for the shift reactor is set to 2.0 for all three systems.

A heater is employed to heat the reactants to a temperature sufficient to sustain the catalytic reaction in the reforming reactor. The outlet temperature of the heater is set to 400 °C for the SMR, 312 °C for the POX and 400 °C for the ATR system, according to the favourable operating conditions. The equilibrium of each reforming reactor is calculated using the same methods as those used before to investigate the equilibrium state. The synthesis gas (syngas) produced by each reforming reactor contains a large amount of CO together with hydrogen. To convert this CO to hydrogen, a water–gas shift reactor is used as described above. The simulation uses only one low-temperature shift reactor to simplify the comparison. It is assumed that this low-temperature shift reactor converts all CO to hydrogen with a conversion of over 0.99. Before the shift reactor, a heat exchanger is employed to cool down the temperature of syngas exhausted from the reforming reactor, which is around 800 °C. The syngas is cooled to the operating temperature of the shift reactor (200 °C). The shift reactor is modelled with the 'Requil' model in AspenPlus™. The material and energy balances for each system are listed in

Table 2
Material and energy balances of each stream in SMR reformer system

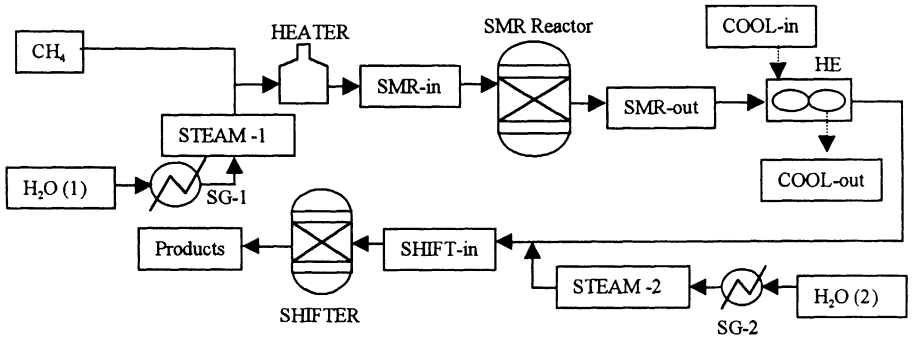

Stream	CH_4	H_2O (1)	STEAM-1	SMR-in	SMR-out	COOL-in	COOL-out	H_2O (2)	STEAM-2	SHIFT-in	Products
Mole flow (mol s^{-1})											
CH_4	0.2526	0	0	0.2526	2.283E−3	0	0	0	0	2.283E−3	2.283E−3
O_2	0	0	0	0	0	0	0	0	0	0	0
N_2	0	0	0	0	0	0	0	0	0	0	0
H_2	0	0	0	0	0.8002	0	0	0	0	0.8001	0.9991
H_2O	0	0.4799	0.4799	0.4799	0.1804	10.0	10.0	0.5052	0.5052	0.1803	0.4866
CO	0	0	0	0	0.2010	0	0	0	0	0.2010	2.155E−3
CO_2	0	0	0	0	0.0492	0	0	0	0	0.0492	0.2489
Mole fraction											
CH_4	1.00	0	0	0.3448	1.852E−3	0	0	0	0	1.852E−3	1.313E−3
O_2	0	0	0	0	0	00	0	0	0	0	0
N_2	0	0	0	0	0	0	0	0	0	0	0
H_2	0	0	0	0	0.6488	0	0	0	0	0.6488	0.5744
H_2O	0	1.00	1.00	0.6552	0.1462	1.00	1.00	1.00	1.00	0.1462	0.2798
CO	0	0	0	0	0.1630	0	0	0	0	0.1630	1.239E−3
CO_2	0	0	0	0	0.0399	0	0	0	0	0.0399	0.1431
Total flow (mol s^{-1})	0.2526	0.4799	0.4799	0.7325	1.2331	10.0	10.0	0.5052	0.5052	1.2331	1.7391
Temperature (K)	293	293	376	673	1073	293	324	293	376	473	473
Pressure (bar)	1.0	1.0	1.0	1.0	1.0	1.0	1.0	1.0	1.0	1.0	1.0
Enthalpy (J mol^{-1})	−7.469E+4	−2.862E+5	−2.394E+5	−1.695E+5	−4.463E+4	−2.862E+5	−2.838E+5	−2.862E+5	−2.394E+5	−6.393E+4	−1.185E+5

HE, heat exchanger; SG, steam generator.

Table 3
Material and energy balances of each stream in POX reformer system

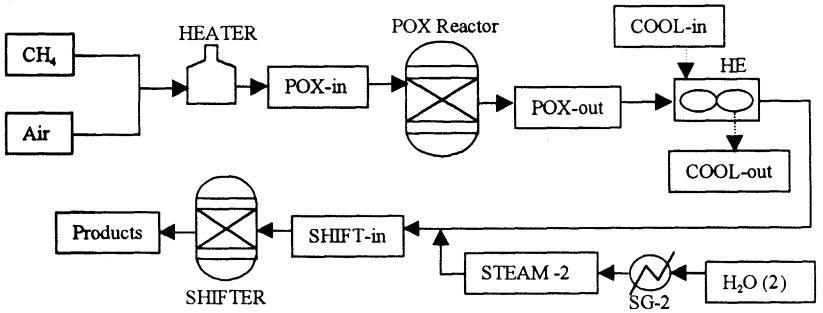

Stream	Air	CH_4	POX-in	POX-out	COOL-in	COOL-out	H_2O (2)	STEAM-2	SHIFT-in	Products
Mole flow (mol s^{-1})										
CH_4	0.0	0.3630	0.3630	3.203E−3	0	0	0	0	3.203E−3	3.203E−3
O_2	0.2178	0	0.2178	0.00	0	0	0	0	0.00	0.00
N_2	0.8218	0	0.8218	0.8218	0	0	0	0	0.8218	0.8218
H_2	0	0	0	0.6702	0	0	0	0	0.6702	1.0002
H_2O	0	0	0	0.0493	10.00	10.00	0.7260	0.7260	0.0493	0.4453
CO	0	0	0	0.3333	0	0	0	0	0.3333	3.389E−3
CO_2	0	0	0	0.0264	0	0	0	0	0.0264	0.3578
Mole fraction										
CH_4	0	1.00	0.2588	1.681E−3	0	0	0	0	1.681E−3	1.217E−3
O_2	0.2095	0	0.1552	0	0	0	0	0	0.00	0.00
N_2	0.7904	0	0.5859	0.4315	0	0	0	0	0.4321	0.3122
H_2	0	0	0	0.3519	0	0	0	0	0.3519	0.3800
H_2O	0	0	0	0.0259	1.00	1.00	1.00	1.00	0.0259	0.1692
CO	0	0	0	0.1750	0	0	0	0	0.1750	1.287E−3
CO_2	0	0	0	0.0138	0	0	0	0	0.0138	0.1359
Total flow (mol s^{-1})	1.0396	0.3630	1.4026	1.9043	10.00	10.00	0.7260	0.7260	1.9043	2.6318
Temperature (K)	293	293	585	1075	293	340	293	376	473	473
Pressure (bar)	1.0	1.0	1.0	1.0	1.0	1.0	1.0	1.0	1.0	1.0
Enthalpy (J mol^{-1})	−1.458E+2	−7.469E+4	−9.764E+3	−7.191E+3	−2.862E+5	−2.826E+5	−2.862E+5	−2.394E+5	−2.604E+4	−8.912E+4

HE, heat exchanger; SG, steam generator.

Table 4
Material and energy balances of each stream in ATR reformer system

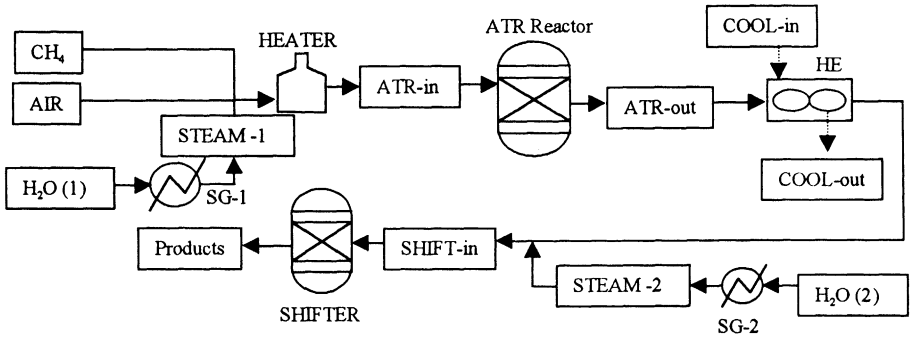

Stream	AIR	CH_4	H_2O (1)	STEAM-1	ATR-in	ATR-out	COOL-in	COOL-out	H_2O (2)	STEAM-2	SHIFT-in	Products
Mole flow (mol s^{-1})												
CH_4	0	0.3546	0	0	0.3546	2.797E−3	0	0	0	0	2.797E−3	2.797E−3
O_2	0.2021	0	0	0	0.2021	0	0	0	0	0	0	0
N_2	0.7627	0	0	0	0.7627	0.7627	0	0	0	0	0.7627	0.7627
H_2	0	0	0	0	0	0.6926	0	0	0	0	0.6926	0.9999
H_2O	0	0	0.07092	0.07092	0.07092	0.0818	10.00	10.00	0.7092	0.7092	0.0818	0.4837
CO	0	0	0	0	0	0.3103	0	0	0	0	0.3103	0.0030
CO_2	0	0	0	0	0	0.0414	0	0	0	0	0.0414	0.3502
Mole fraction												
CH_4	0	1.00	0	0	0.2550	1.478E−3	0	0	0	0	1.478E−3	1.075E−3
O_2	0.2094	0	0	0	0.1453	0	0	0	0	0	0	0
N_2	0.7905	0	0	0	0.5485	0.4031	0	0	0	0	0.4031	0.2930
H_2	0	0	0	0	0	0.3661	0	0	0	0	0.3661	0.3842
H_2O	0	0	1.00	1.00	0.0510	0.0432	1.00	1.00	1.00	1.00	0.0432	0.1858
CO	0	0	0	0	0	0.1640	0	0	0	0	0.1640	1.173E−3
CO_2	0	0	0	0	0	0.0219	0	0	0	0	0.0219	0.1345
Total flow (mol s^{-1})	0.9468	0.3546	0.07092	0.07092	1.3903	1.8918	10.00	10.00	0.7092	0.7092	1.8918	2.6025
Temperature (K)	293	293	293	376	673	1061	293	339	293	376	473	473
Pressure (bar)	1.0	1.0	1.0	1.0	1.0	1.0	1.0	1.0	1.0	1.0	1.0	1.0
Enthalpy (J mol^{-1})	−1.458E+2	−7.469E+4	−2.862E+5	−2.394E+5	−1.850E+4	−1.359E+4	−2.862E+5	−2.826E+5	−2.862E+5	−2.394E+5	−3.213E+4	−9.257E+4

HE, heat exchanger; SG, steam generator.

Tables 2–4. A summary of the material and energy balances for each reforming system is given in Table 5.

The term 'total net energy' in Table 5 means the summation of energy balances of all there units that comprise the reforming system together with consideration of their heat-transfer efficiency. Each unit in a reforming system may, in reality, have a different heat-transfer efficiency but the simulation assumes the same heat-transfer efficiency for all units to simplify the calculation. The term 'CH_4 equivalent' refers to a CH_4 flow rate, the combustion of which will release energy equivalent to the 'total net energy.' A combustion heat of 890 kJ/kmol of CH_4 is used to calculate the CH_4 equivalent from the total net energy. In the table, 'total CH_4' is the sum of 'input' CH_4 and 'CH_4 equivalent.' When considering only the input CH_4, the CH_4 flow rate required to produce 1 mol s^{-1} of hydrogen is 0.253 mol s^{-1} for the SMR, 0.363 mol s^{-1} for the POX and 0.355 mol s^{-1} for the ATR. The total CH_4 flow rate, including the CH_4 equivalent, required to generate 1 mol s^{-1} of hydrogen is 0.385 mol s^{-1} for the SMR, 0.364 mol s^{-1} for the POX and 0.367 mol s^{-1} for the ATR. The SMR reforming system has the highest CH_4 consumption rate and the POX system has the lowest CH_4 consumption rate. One interesting point is that the difference in the CH_4 consumption depends strongly on the heat-transfer efficiency of the heat-exchange units. The difference in CH_4 consumption between the SMR and POX systems becomes larger as the heat-transfer efficiency decreases. For example, when the heat-transfer efficiency is 0.8, the CH_4 consumption is 0.364 mol s^{-1} for the POX and 0.385 mol s^{-1} for the SMR. By contrast, when the heat-transfer efficiency is lowered to 0.7, the values change to 0.364 mol s^{-1} for the POX and 0.404 mol s^{-1} for the SMR.

The results show that, in terms of energy cost, the POX reforming systems is superior to other systems for the production of the same amount of hydrogen from CH_4. If the heat-transfer efficiency of each unit in a reforming system can be improved, then the difference in the rate of CH_4 consumption between the three reforming systems will be reduced. As an extreme case, if the heat-transfer efficiency is 1.0, the SMR system has the lowest energy cost.

Table 5
Comparison of material and energy balances of three reforming systems

	SMR	POX	ATR
Input (mol s^{-1})			
CH_4	0.253	0.363	0.355
O_2	–	0.218	0.202
N_2	–	0.822	0.763
H_2O (1)	0.480	–	0.071
H_2O (2)	0.505	0.726	0.709
Total	1.238	2.129	2.099
Output (mol s^{-1})			
CH_4	0.002	0.003	0.003
O_2	–	0.000	0.000
N_2	–	0.822	0.763
H_2O	0.487	0.445	0.484
CO	0.002	0.003	0.003
CO_2	0.249	0.358	0.350
H_2	1.000	1.000	1.000
CH_4 conversion	0.991	0.991	0.992
CO conversion	0.987	0.990	0.990
Energy balance (kW)			
Heater	9.6	13.6	17.9
Reforming reactor	69.2	0.0	0.0
Heat exchanger	−23.8	−35.9	−35.1
Shift reactor	−6.4	−11.2	−10.3
Steam generator (1)	22.5	0.0	3.3
Steam generator (2)	23.6	34.0	33.2
Heat-transfer efficiency	0.80	0.80	0.80
Total net energy (kW)	118.2	0.6	11.2
CH_4 equivalent (mol s^{-1})	0.133	0.001	0.013
Total CH_4 (input + CH_4 equivalent, mol s^{-1})	0.385	0.364	0.367

4. Conclusions

A thermodynamic analysis has been conducted to investigate the characteristics of three reforming rectors, namely, SMR, POX and ATR. This has allowed identification of the favourable operating conditions for each system. Material and energy balances have also been evaluated for the three reforming systems.

Favourable operating conditions have been determined, which simultaneously satisfy the requirements for no coke formation, a reactor temperature of up to 800 °C and a conversion of over 0.99. The optimum S:C ratio in the SMR reactor is found to be 1.9. For the POX reactor, the optimum conditions include an air ratio of 0.3 and a preheat temperature of 312 °C. The optimum air ratio and S:C ratio in the ATR reactor are 0.29 and 0.35, respectively, at a preheat temperature of 400 °C.

The material and energy balances which result from the simulations for each reforming system show that the total CH_4 flow rate required to generate 1 mol s^{-1} hydrogen is 0.364 mol s^{-1} for the POX, 0.367 mol s^{-1} for the ATR and 0.385 mol s^{-1} for the SMR. The SMR reforming system has the highest CH_4 consumption and the POX system has the lowest CH_4 consumption. The difference in CH_4 consumption between the three reforming systems depends strongly upon the efficiency of the heat exchangers. The difference in CH_4 consumption between the SMR and POX systems becomes larger as the efficiency of the heat exchangers decreases. When the heat-transfer efficiency is 0.8, the CH_4 consumption rates of the POX and SMR systems are 0.364 and 0.385 mol s^{-1} respectively. On the other hand, when the heat-transfer efficiency is lowered to 0.7, these values change to 0.364 mol s^{-1} for the POX and 0.404 mol s^{-1} for the SMR. These evaluations reveal that the POX reforming system is superior to the other systems in terms of the energy cost to produce the same amount of hydrogen from CH_4.

Acknowledgements

This work has been supported by a postdoctoral fellowships program from Korea Science and Engineering Foundation (KOSEF).

References

[1] M.A. Pena, J.P. Gomez, J.L.G. Fierro, Appl. Catal. A: Gen. 144 (1996) 7–57.
[2] R. Wegeng, L.R. Pederson, W.E. TeGrotenhuis, G.A. Whyatt, Fuel Cells Bull. 3 (2001) 8–13.
[3] G. Sattler, J. Power Sources 86 (2000) 61–67.
[4] B. Emonts, J.B. Hansen, H. Schmidt, T. Grube, B. Hohlen, R. Peters, A. Tschauder, J. Power Sources 86 (2000) 228–236.
[5] K.A. Starz, E. Auer, T. Lehmann, R. Zuber, J. Power Sources 84 (1999) 167–172.
[6] T. Susai, A. Kawakami, A. Hamada, Y. Miyake, Y. Azegami, Fuel Cells Bull. 3 (2001) 7–11.
[7] A. Piga, X.E. Verykio, Catal. Today 60 (2000) 63–71.
[8] S.S. Bharadwaj, L.D. Schmidt, Fuel Processing Technol. 42 (1995) 109–127.
[9] K.G. Marnasidou, S.S. Voutetakis, G.J. Tjatjopoulos, I.A. Vasalos, Chem. Eng. Sci. 54 (1999) 3691–3699.
[10] T. Wurzel, L. Mleczko, Chem. Eng. J. 69 (1998) 127–133.
[11] T. Rampe, A. Heinzel, B. Vogel, J. Power Sources 86 (2000) 536–541.
[12] S. Cavallaro, S. Freni, J. Power Sources 76 (1998) 190–196.
[13] V. Recupero, L. Pino, R.D. Leonardo, M. Lagana, G. Maggio, J. Power Source 71 (1998) 208–214.
[14] J. Han, I. Kim, K. Choi, J. Power Sources 86 (2000) 223–227.
[15] S.H. Chan, H.M. Wang, Fuel Processing Technol. 64 (2000) 221–239.
[16] Aspen Technology Inc., http://www.aspentech.com/.
[17] S. Freni, G. Calogero, S. Cavallaro, J. Power sources 87 (2000) 28–38.